Thin Solid Films 519 (2011) 5700–5705

Contents lists available at ScienceDirect

Thin Solid Films

journal homepage: www.elsevier.com/locate/tsf

Thermophysical properties of free-standing micrometer-thick Poly (3-hexylthiophene) films

Xuhui Feng, Xinwei Wang *

Department of Mechanical Engineering, 2010 Black Engineering Building, Iowa State University, Ames, IA 50011, USA

ARTICLE INFO

Article history:
Received 6 October 2010
Received in revised form 8 March 2011
Accepted 16 March 2011
Available online 31 March 2011

Keywords:
Poly(3-hexylthiophene)
Organic semiconductors
Thin films
Thermal conductivity
Density
Transient electro-thermal technique

ABSTRACT

The solution of Poly(3-hexylthiophene) (P3HT) in chloroform is generally adopted for fabricating P3HT thin films or nanofibers. In this work, 4 regular P3HT solution weight percentages, 2, 3, 5 and 7 wt.%, are compounded to fabricate P3HT thin films by using spin-coating technique. Raman spectrum study suggests that the density of the P3HT thin films varies with different P3HT solution weight percentages while X-ray diffraction analysis reveals that the crystal structures are identical for all P3HT thin films. The transient electrothermal technique is employed to measure the thermal diffusivity of the P3HT thin films and an efficient temperature–resistance calibration is performed to cooperatively study the thermal conductivity. When the P3HT weight percentage changes from 2% to 7%, the thermal conductivity varies from 1.29 W/m·K to 1.67 W/m·K and the thermal diffusivity goes down from around 10^{-6} m^2/s to 5×10^{-7} m^2/s. The density of P3HT thin films is also determined from the experimental data. The relationship between the density and thermophysical properties clearly demonstrates that the thermal conductivity increases with density while the thermal diffusivity decreases.

1. Introduction

As a promising organic polymer material, Poly(3-hexylthiophene) (P3HT) has been proven to have advantages over conventional semiconductors in light of weight, processability and environmental sustainability while it still has electrical conducting property similar to semiconductors. This polymer material has become an essential subject of interest for both academic and industrial researchers. Various achievements have been reported regarding its development [1]. Synthesis of P3HT was conducted and significant attentions have been paid on improving the regioregularity and controlling the molecular weight and polydispersities of the fabricated P3HT [2–7]. Although the preparation of P3HT has been widely studied, it is still a complicated chemical or electrochemical process for non-chemistry professionals, not to mention to fabricate P3HT of defined molecular weight or specific regioregularity. The availability of commercial-grade P3HT has substantially boosted in-depth and extensive research on developing various forms of P3HT such as thin films [8–15], microwires [10,15,16] and nanofibers [15,17–22], and also on its electrical, optical and thermal properties in practical applications such as photovoltaic cells and field-effect transistors. In order to determine the density of P3HT film, an atomic force microscopy (AFM) in combination with Rutherford backscattering spectroscopy data was applied and the density was estimated at 1.33 ± 0.07 g/cm^3 [8]. The thermal behavior and morphology transition of P3HT thin films developed by spin-casting were studied by Hugger et al. [9] using X-ray diffraction measurements with AFM data. The transition temperature was found about 225 °C and a layered and smectic liquid crystalline phase of P3HT formed. Another efficient method to promote order–disorder transformation of P3HT in solution by ultrasonic oscillation was presented by Zhao et al. [23]. Upon ultrasonic oscillating, chain entanglements were decreased in the ordered precursors. Four minutes was enough to yield the best crystallinity of the film. The intrinsic photoconductivity of P3HT polymers was measured and conclusion was made that higher mobility is associated with higher molecular weight by using optical pump–THz probe spectroscopy [11]. A study [24] on the molecular structure of P3HT indicated that a rotation of the planes containing the conjugated rings in P3HT substantially contributed to electrical conductance: the rotation reduces the electron and hole bandwidths and opens up the energy gap between occupied and empty states. To enhance the conductance of P3HT, germanium endometallo fullerene was added into P3HT matrix and the temperature is also significant to this adding process for achieving high conductance [25]. In practical applications, P3HT was adopted to synthesize a composite with phenyl-C61-butyric acid methyl ester (PCBM) as the active layer in polymer photovoltaic cells. It was proven that heat treatment dramatically improved the cell's performance. The power conversion efficiency was improved up to 2.8% under white light illumination because the annealing contributed to optimizing both the donor/acceptor morphology [26]. Research by Janssen et al. [12] also revealed the effect of thermal treatments in optimizing the morphology of P3HT/PCBM films for organic solar cells by monitoring the optical absorption and resonant Raman scattering.

* Corresponding author. Tel.: +1 515 294 2085; fax: +1 515 294 3261.
E-mail address: xwang3@iastate.edu (X. Wang).

0040-6090/$ – see front matter © 2011 Elsevier B.V. All rights reserved.
doi:10.1016/j.tsf.2011.03.043

Even though the electrical properties of P3HT have been extensively explored, little work has been reported regarding its thermal properties. The deficiency of thermal diffusion pathways in present compact electrical systems is prone to heat accumulation and performance compromise. Therefore, in-depth investigation on thermal properties of P3HT is crucial to thermal response of P3HT-based devices for identifying a proper working environment. In this work, the spin-coating technique is applied to fabricate P3HT thin films of about 30–50 μm thickness and the thermophysical properties of prepared P3HT thin films are studied systematically. In Section 2, the preparation and optical examination of P3HT thin films are introduced followed by a brief introduction of transient electro-thermal (TET) technique for thermal characterization. All measured data and related discussion are presented in Section 3 to show the relevance between thermal and physical properties of the P3HT thin films.

2. Experimental details

2.1. Sample preparation

Regioregular P3HT (average molecular weight = 50,000 MW) is purchased from Rieke Metals and anhydrous chloroform is obtained from Sigma Aldrich. As-purchased compounds are used without further processing. Preparation of the P3HT solution is conducted in an argon glove compartment and the solution is then magnetically stirred in a capped vial for 1 h, with auxiliary heating up to 50 °C to help dissolve. The P3HT thin film is prepared in air by spin-coating at 5000 rpm for 45 s in a Pyrex glass dish. Thickness of the P3HT thin film may slightly vary from spot to spot because the bottom of the dish is not absolutely flat. Although P3HT is a conductive polymer material, the relatively poor electrical conductivity is not sufficient for acquiring strong signal in our thermal characterization experiment. Therefore after the P3HT thin film is removed from the dish, it is coated with an ultra-thin gold layer for conducting electric current and thermal sensing purpose. The coating procedure is done using a Denton vacuum sputtering device and continued for 100 s, which is estimated to generate a gold coating of 50 nm thickness. Further discussion will be given later to examine the influence of the gold coating on thermophysical property measurement. In order to identify the crystal structure of the P3HT thin film, Voyage confocal Raman spectroscopy is used and a comparison of typical Raman spectra of the prepared P3HT thin films is presented in Fig. 1, with an excitation laser of 532 nm wavelength, 0.2 mW power and $3\times10\ \mu m^2$ spot size. An integration time of 30 s is chosen for all samples. The samples are all placed with the surface facing the laser beam perpendicularly. Under consistent working conditions, it can be observed that for P3HT films fabricated from solutions of different P3HT weight percentages, the Raman spectra follow similar distributions and the characteristic bands are distinctly observed for every P3HT thin film, while the intensity varies with P3HT solution weight percentage. Among all spectra, the band with a maximum value around 1448 cm^{-1} is related to the $C_\alpha{=}C_\beta$ bond of the thiophene ring, while the other peak around 1382 cm^{-1} represents the $C_\alpha{-}C_\beta$ bond stretching [27]. The exact value of the peaks for different films may be moderately different but close enough. Under identical integration time higher P3HT solution weight percentage gives sharper and more distinct peaks. For the Raman spectrum peak height, it is proportional to $[1-\exp(-2z_0/\tau)]$ where z_0 is the film thickness and τ is the optical absorption depth. τ is proportional to the inverse of film density (ρ). As will be discussed later (Fig. 5), when the P3HT solution weight percentage is higher during fabrication, the fabricated film is thicker and has a higher density. This explains why the higher P3HT solution weight percentage in fabrication gives higher Raman peak intensity.

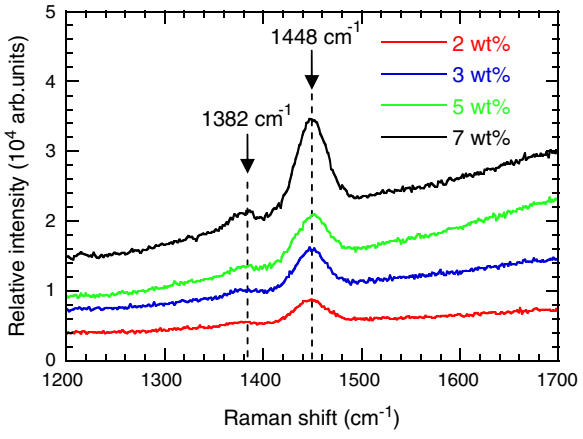

Fig. 1. Comparison of Raman spectrum of P3HT thin films fabricated with different P3HT solution weight percentages.

2.2. Electrical resistance (R) temperature coefficient calibration

For Au-coated P3HT thin films, the electrical conductance and thermal conductance are significantly enhanced compared with bare samples. A calibration procedure is conducted before the TET measurement to determine the temperature coefficient of resistance for the P3HT thin films. The Au-coated P3HT thin film is suspended between two aluminum electrodes by silver paste and a K-type thermocouple is attached to measure the temperature change of the P3HT thin film. Although the thermocouple is pasted to the electrode surface, an assumption is made that the temperature readings represent the P3HT thin film's temperature since the film is very short and tightly connected to the electrodes. The calibration procedure is conducted in a vacuum chamber whose pressure is kept lower than 0.13 Pa to reduce unnecessary heat conduction to air. During the calibration, a DC voltage of about 44 V is engaged for the heater placed under the stage and the temperature variation during calibration is controlled between 25 °C and 60 °C to avoid potential damage to the P3HT thin film. Temperature and resistance readings during the cooling phase are collected because in the cooling phase there is no heat generation in the heater and the heat transfer is relatively slow compared to the heating process. Therefore the collected temperature can be assumed the evenly-distributed temperature of the suspended P3HT thin film.

2.3. TET experimental principles

The TET technique [28] is a fast and efficient approach to measuring the thermal diffusivity of solid materials, including conductive, semi-conductive or even non-conductive materials. A schematic of TET experiment setup is shown in Fig. 2(a). It is performed immediately after the temperature–resistance calibration procedure. During the TET experiment, a step DC current (I) is fed through the P3HT thin film to generate electrical heat. The transient temperature increase of the P3HT thin film is strongly dependent on the heat transfer within the film and it then leads to resistance change and induces an overall voltage change. The voltage change of P3HT thin film under the fed DC current is collected by an oscilloscope for further data process. A fed current–time (I–t) profile and an induced voltage–time (V–t) profile recorded by the oscilloscope are presented in Fig. 2(b). As explained in this figure, under the feeding of square current (black dashed line), the induced voltage profile (red solid line) undergoes a rapid increase phase and then reaches the steady state, meaning heat transfer equilibrium is achieved. The transient phase can be used to determine the thermal diffusivity and the voltage difference between initial and steady states can be used to determine the thermal conductivity. Under our experimental conditions, the physical model of the TET technique is simplified to a one-dimensional heat conduction problem and more details can be referred to Guo's work [28]. With the calibrated temperature coefficient of

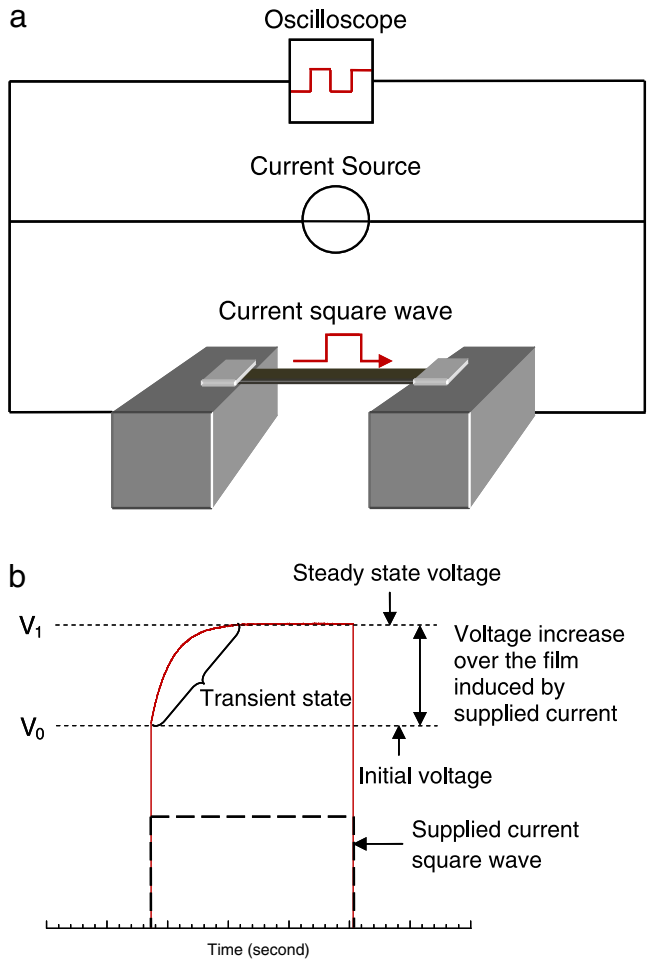

Fig. 2. (a) Schematic of the experimental principle and the step current provided for the TET technique, and (b) fed current (black dash line) and methodology to determine the thermophysical properties based on the resulted V–t profile (red solid line).

resistance η and the resistance change ΔR during the transient state, the temperature change ΔT is calculated and then the thermal conductivity (k) is obtained as $k = I^2RL/(12A\Delta T)$. A and L are the cross-sectional area and the length of the film, respectively. The normalized temperature increase (T^*) is solved for a one-dimensional heat transfer problem,

$$T^* = \frac{96}{\pi^4}\sum_{m=1}^{\infty}\frac{1-exp\left[-(2m-1)^2\pi^2\alpha t/L^2\right]}{(2m-1)^4}. \quad (1)$$

The voltage evolution (V_{film}) recorded by the oscilloscope is directly related to the average temperature change of the P3HT thin film as

$$V_{film} = IR_0 + I\eta\frac{8q_0L^2}{k\pi^4}\times\sum_{m=1}^{\infty}\frac{1-exp\left[-(2m-1)^2\pi^2\alpha t/L^2\right]}{(2m-1)^4}, \quad (2)$$

where V_{film} is the recorded overall voltage of the P3HT thin film, and R_0 is the resistance of the P3HT thin film before heating. It is clear that the measured voltage change is inherently related to the temperature change of the P3HT thin film.

However, the measured thermal diffusivity (α_e) is only an effective value combining both effects of the P3HT thin film and the gold coating because the tested P3HT thin film is already coated with a thin gold layer to enhance the electrical conduction. The thermal transfer effect caused by the coated layer can be subtracted using the Lorenz number without increasing the uncertainty. The real thermal diffusivity (α) of the P3HT thin film is determined as

$$\alpha = \alpha_e - \frac{L_{Lorenz}TL}{RA_w\rho c_p}, \quad (3)$$

where ρ and c_p are the effective density and the specific heat of the sample, respectively and L_{Lorenz} is the Lorenz number. With known parameters, this modification is effective to eliminate the effect of the gold coating. The real thermal conductivity can also be determined following the similar methodology and is derived as,

$$k = k_e - \frac{L_{Lorenz}TL}{RA_w}. \quad (4)$$

In order to practically determine the real thermal diffusivity and thermal conductivity, physical parameters such as density and specific heat are required besides the effective thermophysical parameters, dimensional parameters and temperature. The effective density is acquired according to the expression of thermal diffusivity, $\alpha = k/\rho c_p$, after determining the thermophysical parameters experimentally and referring to literature for the value of specific heat. Then based on Eqs. (3) and (4), the real thermophysical properties are obtained. More details about this methodology will be demonstrated in the following.

3. Results and discussion

3.1. TET measurement of thermal conductivity and thermal diffusivity

All prepared P3HT thin films are about 20–50 μm thick. The thickness measurement has about 10% uncertainty and its impact on the final results will be discussed later. In this section, a selected P3HT thin film is chosen to demonstrate the experiment and post-processing procedure. All details of this film are listed in Table 1 while a microscopic image is presented in Fig. 3(a) to show its real dimension during the measurement.

As discussed in Guo's work [28], theoretical fitting of the normalized experimental temperature rise (expressed by Eq. (1)) is conducted by using different trial values of the thermal diffusivity of the sample. The value giving the best fit of the experimental data is taken as the property of the film. Fitting of the experimental data for this film is illustrated in Fig. 3(b) and the thermal diffusivity is determined at 8.06×10^{-7} m^2/s, which still includes the influence of the gold coating layer. Based on Eq. (3), both the density and specific heat of this material are required to evaluate this influence. Calorimetric measurements revealed that for regioregular P3HT an endothermic transition from a crystalline to a liquid crystalline state occurs at 210–225 °C [9]. However, because of the low temperature range during our experiment, the endothermic transition is not considered and the specific heat is around 1550–1620 J/kg·K, depending on the specific temperature of the P3HT film [9].

Table 1
Details of experimental parameters and results for a selected P3HT thin film characterized by using the TET technique.

Length (mm)	3.66
Width (mm)	0.29
Thickness (μm)	33.0
Resistance (Ω)	34.0
DC current (mA)	6.00
Weight percentage (wt.%)	3.00
Effective density (kg/m^3)	1200
Measured thermal diffusivity ($\times10^{-7}$ m^2/s)	8.06
Real thermal diffusivity ($\times10^{-7}$ m^2/s)	7.64
Effective thermal conductivity (W/m·K)	1.57
Real thermal conductivity (W/m·K)	1.48

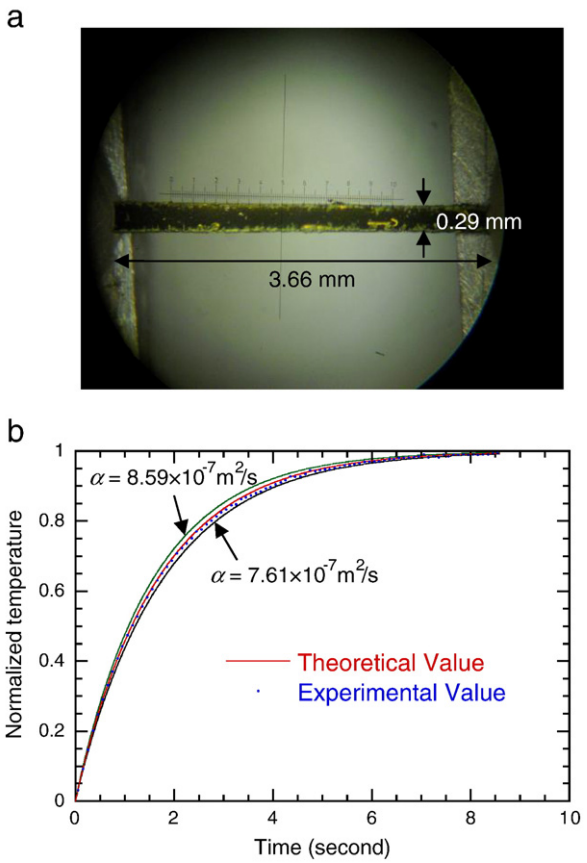

Fig. 3. (a) Microscopic image of the selected P3HT thin film listed in Table 1, and (b) comparison between the theoretical fitting and experimental data for the normalized temperature rise versus time.

According to Erwin's work, the density of the P3HT thin film can be derived based on film thickness and the molecular weight of a P3HT monomer and the average value of density for the P3HT thin film is determined at 1.33 ± 0.07 g/cm^3 [8] by measuring the thickness and combining the Rutherford backscattering spectroscopy data. Nevertheless, in this work the density of every P3HT thin film is individually estimated using obtained thermal conductivity, thermal diffusivity and specific heat based on the definition of the thermal diffusivity, $\alpha = k/\rho c_p$. The thermal conductivity of the P3HT thin film is calculated from the calibration procedure of the temperature coefficient of resistance η. As analyzed before, the heating and temperature range is moderate to assure that the P3HT thin film is intact, and a typical calibration profile of the P3HT thin film in Table 1 is displayed in Fig. 4. A distinct linear temperature–resistance relationship similar to an excellent conductor is presented because the gold coating strongly enhances the electrical conduction of the P3HT thin film. A linear fitting is used to obtain the temperature coefficient of resistance, which is 3.04×10^{-2} Ω/K for this P3HT thin film. With 6 mA DC current passing through this film, the resistance change is calculated to be 0.76 Ω and the consequent temperature change is 25.1 K, which is in the expected temperature variation range and assures the P3HT thin film undamaged during the experiment procedure. The thermal conductivity is derived based on previous expression as 1.57 W/m·K. Then the effective density of the P3HT thin film in Table 1 is calculated to be 1200 kg/m^3, which is close to the literature value considering the measurement uncertainty.

The thermal diffusivity and thermal conductivity for calculating the density are both effective values that include the effect of gold coatings. In order to rule out the impact, modification is performed with known dimensional parameters and physical properties. The real thermal diffusivity is 7.64×10^{-7} m^2/s and the real thermal conductivity is 1.48 W/m·K based on Eqs. (3) and (4), implying that the impact of gold coating is small (around 5%). The obtained thermal conductivity is higher than the typical value for a polymer material that is less than 1 W/m·K.

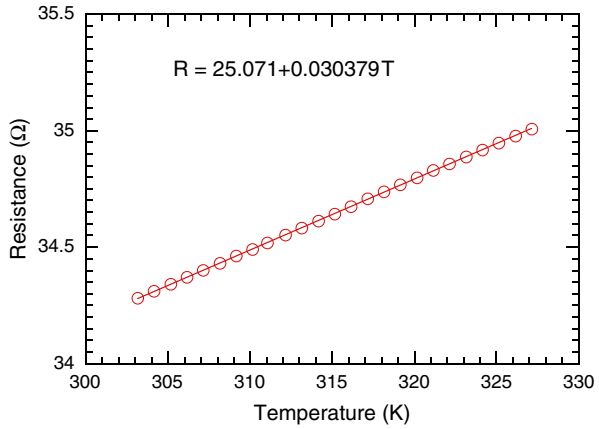

Fig. 4. Linear fitting curve of the temperature coefficient of resistance for the P3HT thin film in Table 1.

3.2. Thermophysical properties of P3HT thin films with different dimensions

P3HT thin films fabricated from solutions of different P3HT weight percentages are measured to explore the relationship between the weight percentage and thermophysical properties. However, even though under the same weight percentage, the internal structure of fabricated samples may still have slight difference and therefore the measured data from the same weight percentage are treated separately instead of studying the average values. The obtained data still demonstrate a certain trend when minor deviations exist within the data from the same weight percentages. Detailed information about all P3HT thin films is listed in Table 2, along with the real thermophysical properties and effective density. The thermal conductivity and diffusivity in Table 2 are the values exclusive of gold coating effect. Because of different P3HT solution weight percentages, the density of spin-coated P3HT thin films is different, varying from 878 to 1640 kg/m^3 while the literature value is around 1330 kg/m^3 [8]. This variation is supported by the Raman spectra shown in Fig. 1 in which it can be seen that higher P3HT solution weight percentage contributes to more distinct band. When the weight percentage increases from 2 wt.% to 7 wt.%, the average density of all P3HT thin films at each weight percentage increases from 954 kg/m^3 to 1520 kg/m^3. Higher weight percentage gives higher density while the values around 7 wt.% have deviations which may be attributed to the uncertainty introduced by thermal conductivity measurement. The thickness is also believed to be impacted by the P3HT solution weight percentage. When it changes as 2, 3, 5 and 7 wt.%, the average thickness of P3HT thin films at each solution weight percentage is measured at 24, 26, 37 and 42 μm, respectively. When measuring the thickness by using a micrometer caliper, because of the flexibility of P3HT films, three measurements are performed for each film to obtain an average value which has about 10% uncertainty in the thickness measurement. The flatness of the film surface varies from spot to spot because of the quick spin-coating process and different weight percentages. Surface flatness is an important factor to induce uncertainties into the thickness measurement, which consequently impacts the measured thermal properties. When preparing the P3HT solution, higher weight percentage gives higher viscosity of the solution. Therefore during the spin-coating procedure, thicker film is fabricated with higher viscosity. Detailed relation between the thickness, density and the P3HT weight percentage during fabrication is illustrated in Fig. 5.

Table 2
Experimental data and calculated results of all P3HT thin films examined in this work.

Sample #	Length (mm)	Width (mm)	Thickness (μm)	wt.%	DC current (mA)	$\Delta R/\Delta T$ (Ω/K)	Effective density (kg/m^3)	Thermal diffusivity ($\times 10^{-7}$ m^2/s)	Thermal conductivity (W/m·K)
1	2.60	0.23	26.0	2.00	6.00	52.1	878	9.00	1.29
2	2.65	0.43	22.0	2.00	8.00	56.7	1030	8.79	1.45
3	3.24	0.29	18.0	3.00	5.00	43.1	935	10.3	1.55
4	3.66	0.29	33.0	3.00	6.00	32.9	1200	7.64	1.48
5	3.05	0.50	35.0	5.00	5.00	16.1	1590	6.14	1.57
6	2.98	0.39	39.0	5.00	5.00	16.1	1640	6.33	1.67
7	3.32	0.42	31.0	7.00	8.00	40.1	1470	6.79	1.59
8	2.14	0.32	52.0	7.00	15.0	129.7	1570	5.75	1.44

Fig. 6(a) shows the variation of thermal conductivity and thermal diffusivity versus the P3HT solution weight percentage. For thermal conductivity, it shows insignificant change but only slight vibration around 1.5 W/m·K with average deviation less than 15%. Therefore considering the measurement uncertainty, this deviation is not distinct and the P3HT solution weight percentages can be concluded to have little influence on the thermal conductivity. On the other hand, the thermal diffusivity shows significant impact from the P3HT solution weight percentages. When the weight percentage ascends from 2 wt.% to 7 wt.%, the thermal diffusivity descends from 8.90×10^{-7} to 6.27×10^{-7} m^2/s. This decrease of the thermal diffusivity is mostly induced by the density increase as shown in Fig. 5. An X-ray diffraction (XRD) analysis performed using Siemens D500 is presented in Fig. 6(b). 3 peaks are observed at 5.4, 10.8 and 16.3°. The X-ray diffractometer was operated using the Cu tube at 45 kV and 30 mA, and the diffracted beam monochromator was tuned to Cu K-alpha radiation. From the separation of each peak, it can be identified that the three peaks represent three parallel crystal planes, each of which can be reasonably assigned to the (001), (002) and (003) plane, respectively. A single spacing separation is calculated to be 16.4 Å [29] from XRD data. The XRD of all P3HT thin films indicates that with different P3HT solution weight percentages the XRD profiles follow same peak values and plane separations. It means that the crystal structure of all P3HT thin films fabricated from the P3HT solution of different weight percentages does not demonstrate distinct difference.

In Fig. 7 the relationships between density and thermal diffusivity and thermal conductivity are presented. Because the structure of fabricated P3HT films embraces loose nature, density may vary distinctly dependent on the fabrication conditions and it becomes an important physical property of P3HT. Compared with the P3HT solution weight percentage, the density proves to be a better parameter to study the variation of thermal conductivity and thermal diffusivity. The thermal conductivity slightly increases from 1.29 W/m·K to 1.67 W/m·K with density increase. The variation range of thermal conductivity is about 30% within the density scope. Although the impact of density on the thermal diffusivity is also not strong, the thermal diffusivity shows contrary influence from density when it decreases from 1.03×10^{-6} to 5.75×10^{-7} m^2/s with little deviation. It can be concluded that although density affects both thermophysical properties, the tendencies are different. Thermal conductivity only relies on the amount of phonons and the scattering process inside the material. Undoubtedly with similar crystal structures higher density means less cavity and higher thermal conductivity. On the other hand, the thermal diffusivity is a ratio of the material's ability to conduct thermal energy over the capability to store thermal energy. The effect of density on storing energy is more than that on increasing thermal conductivity. The comprehensive effect is that the thermal diffusivity decreases with increasing density, which is contrary to the trend of thermal conductivity. Compared with the P3HT solution weight percentage,

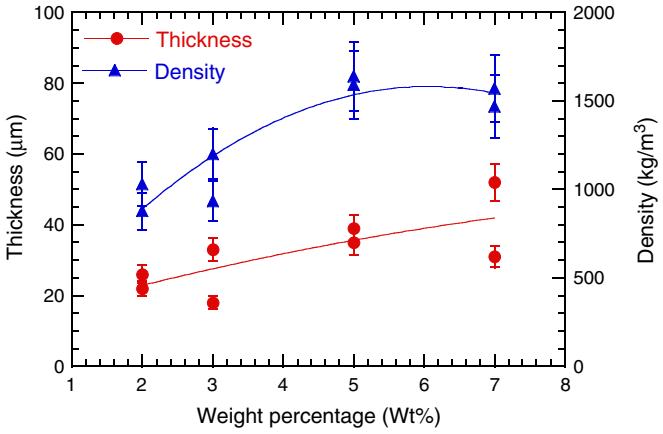

Fig. 5. Thickness and density of P3HT thin films versus the P3HT solution weight percentage. The curves are used to guide eyes to view the data trend.

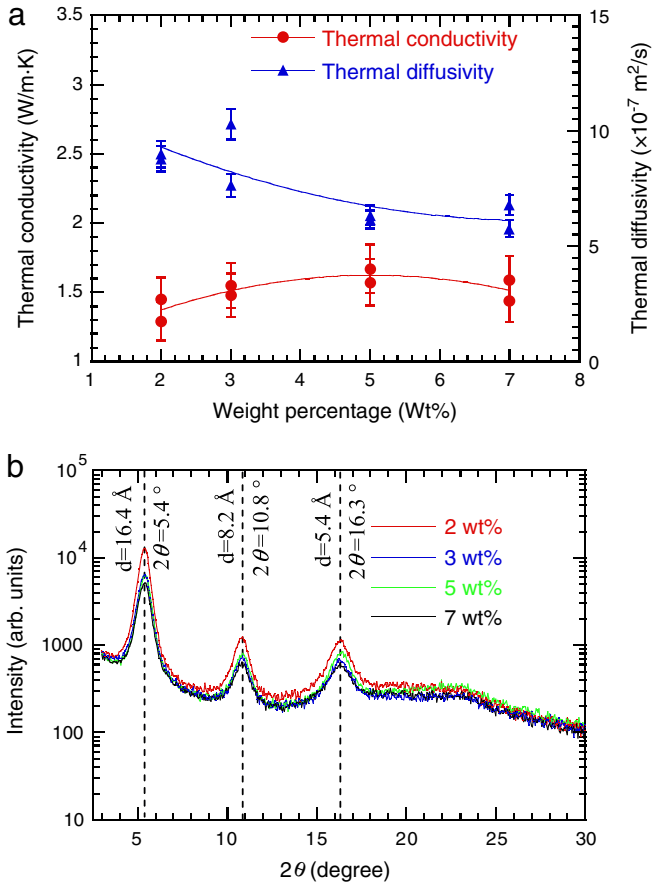

Fig. 6. (a) Thermal conductivity and thermal diffusivity of P3HT thin films versus the P3HT solution weight percentage while the curves are used to guide eyes to view the data trend, and (b) XRD analysis of P3HT thin films fabricated from solutions of different weight percentages.

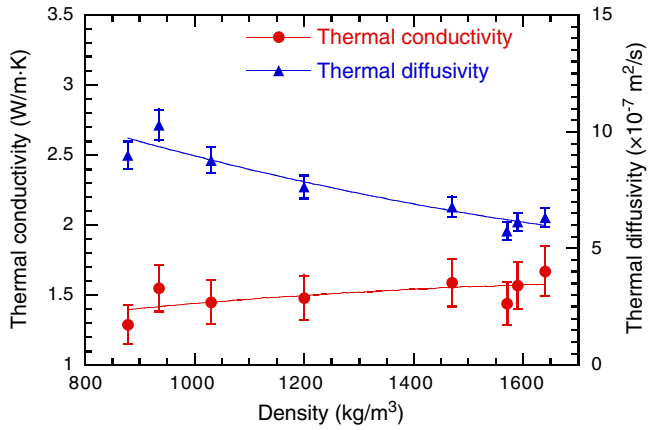

Fig. 7. Thermal conductivity and thermal diffusivity versus the density of the P3HT thin films listed in Table 2. The curves are used to guide eyes to view the data trend.

density exhibits stronger influence on the variation tendency of the thermophysical properties. In Fig. 6(a), the profiles can be simply interpreted as variations within a certain range while in Fig. 7 the profiles give more distinct tendencies with changing parameters. Because the crystal structures are identical for all P3HT thin films, and the P3HT solution of same weight percentage probably yields different densities, the density can be treated as a more representative factor to explain the thermophysical property difference among all P3HT thin films.

For uncertainty assessment purpose, error bars are also shown in Figs. 5, 6(a) and 7. As analyzed before in this section, the major contributor of uncertainties is the measurement of dimensions, especially the thickness. Although the deformation caused by micrometer caliper is usually just 1–2 μm, it is not negligible in this experiment because the film is only around 20–50 μm thick. Therefore the maximum measurement uncertainty from the thickness is evaluated to be about 10%, as shown by the error bars in Fig. 5. For film length and width, they are read directly from the pictures taken by microscope and the uncertainties are about 1%. All experimental devices and equipment, such as the constant current source, oscilloscope and digital multi-meter are calibrated before the measurement. Therefore the uncertainties from current and resistance readings are negligible. From the equation to calculate effective thermal conductivity, the total uncertainty of k is about 10.1%, demonstrating that the largest uncertainty is from the measurement of thickness.

For thermal diffusivity, it is directly measured with the TET technique and the uncertainty is estimated to be 6% as shown by the other two profiles in Fig. 3(b). This value is determined by changing the thermal diffusivity to examine if any distinct deviation of the fitting occurs from the experimental data. With thermal conductivity and thermal diffusivity, the uncertainty of density can also be derived and is estimated to be around 12% according to error propagation theory. After obtaining the uncertainties of all necessary variables, the uncertainties of real thermal diffusivity and real thermal conductivity are calculated to be 6.4% based on Eq. (3) and 10.7% based on Eq. (4) after subtracting the impact of gold coating. Error bars for both thermal properties are added in Figs. 6(a) and 7.

4. Conclusion

P3HT thin films were fabricated using spin coating technique from solution of different P3HT weight percentages: 2%, 3%, 5% and 7%. The TET technique combined with a temperature–resistance calibration procedure was employed to determine the thermophysical properties. The P3HT solution of different weight percentages in fabrication contributed to different physical properties, such as thickness and density. The thickness of spin-coated P3HT thin film was tens of micrometers and the density varies from 878 to 1640 kg/m^3. Considering the included measurement uncertainty, average thickness and density at each solution weight percentage were positively affected by the P3HT solution weight percentage. The thermophysical properties were also influenced by the P3HT solution weight percentage and density. The thermal diffusivity decreased from 1.03×10^{-6} to 5.75×10^{-7} m^2/s with increasing the P3HT solution weight percentage while the thermal conductivity presented only moderate influence from the P3HT solution weight percentage. Compared with the P3HT solution weight percentage, the final film density is a more representative parameter to study the variation of thermal diffusivity and thermal conductivity. The film thermal conductivity increased with density while the thermal diffusivity decreased. The thermal diffusivity decrease demonstrated that the effect of density on storing energy is more than that on increasing thermal conductivity.

Acknowledgment

Support of this work from the National Science Foundation (CBET-0931290) is gratefully acknowledged.

References

[1] J. Roncali, Chem. Rev. 92 (1992) 711.
[2] T.A. Chen, R.D. Rieke, J. Am. Chem. Soc. 114 (1992) 10087.
[3] T.A. Chen, X.M. Wu, R.D. Rieke, J. Am. Chem. Soc. 117 (1995) 233.
[4] R.S. Loewe, S.M. Khersonsky, R.D. McCullough, Adv. Mater. 11 (1999) 250.
[5] E.E. Sheina, J.S. Liu, M.C. Iovu, D.W. Laird, R.D. McCullough, Macromolecules 37 (2004) 3526.
[6] A. Yokoyama, R. Miyakoshi, T. Yokozawa, Macromolecules 37 (2004) 1169.
[7] A. Yokoyama, A. Kato, R. Miyakoshi, T. Yokozawa, Macromolecules 41 (2008) 7271.
[8] M.M. Erwin, J. McBride, A.V. Kadavanich, S.J. Rosenthal, Thin Solid Films 409 (2002) 198.
[9] S. Hugger, R. Thomann, T. Heinzel, T. Thurn-Albrecht, Colloid. Polym. Sci. 282 (2004) 932.
[10] D.H. Kim, Y.D. Park, Y. Jang, S. Kim, K. Cho, Macromol. Rapid Comm. 26 (2005) 834.
[11] O. Esenturk, J.S. Melinger, E.J. Heilweil, 2007 Conference on Lasers & Electro-Optics/Quantum Electronics and Laser Science Conference (Cleo/Qels 2007), Vols 1–5, 2007, p. 2743.
[12] G. Janssen, A. Aguirre, E. Goovaerts, P. Vanlaeke, J. Poortmans, J. Manca, Eur. Phys. J. Appl. Phys. 37 (2007) 287.
[13] A. Khaliq, F.L. Xue, K. Varahramyan, Microelectron. Eng. 86 (2009) 2312.
[14] G. Scavia, W. Porzio, S. Destri, A.G. Schieroni, F. Bertini, E-Polymers (2009) 1.
[15] R. Gonzalez, N.J. Pinto, Synth. Met. 151 (2005) 275.
[16] D.H. Kim, J.T. Han, Y.D. Park, Y. Jang, J.H. Cho, M. Hwang, K. Cho, Adv. Mater. 18 (2006) 719.
[17] T.J. Savenije, J.E. Kroeze, X.N. Yang, J. Loos, Thin Solid Films 511 (2006) 2.
[18] A. Laforgue, L. Robitaille, Synth. Met. 158 (2008) 577.
[19] C.C. Kuo, C.T. Wang, W.C. Chen, Macromol. Symp. 279 (2009) 41.
[20] S. Lee, G.D. Moon, U. Jeong, J. Mater. Chem. 19 (2009) 743.
[21] N.J. Pinto, K.V. Carrasquillo, C.M. Rodd, R. Agarwal, Appl. Phys. Lett. 94 (2009) 083504.
[22] S.W. Lee, H.J. Lee, J.H. Choi, W.G. Koh, J.M. Myoung, J.H. Hur, J.J. Park, J.H. Cho, U. Jeong, Nano Lett. 10 (2010) 347.
[23] K. Zhao, L.J. Xue, J.G. Liu, X. Gao, S.P. Wu, Y.C. Han, Y.H. Geng, Langmuir 26 (2010) 471.
[24] J.E. Northrup, Phys. Rev. B 76 (2007) 245202.
[25] D. Roy, N.K. Tripathi, A. Saraiya, K. Ram, J. Appl. Polym. Sci. 114 (2009) 491.
[26] H. Kim, W.W. So, S.J. Moon, J. Korean Phys. Soc. 48 (2006) 441.
[27] M. Baibarac, M. Lapkowski, A. Pron, S. Lefrant, I. Baltog, J. Raman Spectrosc. 29 (1998) 825.
[28] J.Q. Guo, X.W. Wang, T. Wang, J. Appl. Phys. 101 (2007) 063537.
[29] K. Sugiyama, T. Kojima, H. Fukuda, H. Yashiro, T. Matsuura, Y. Shimoyama, Thin Solid Films 516 (2008) 2691.